

Supporting information for: Activity Coefficients and Solubility of CaCl_2 from Molecular Simulations

Jeffrey M. Young,[†] Christopher Tietz,[‡] and Athanassios Z. Panagiotopoulos^{*,†}

[†]*Department of Chemical and Biological Engineering, Princeton University, Princeton,
New Jersey 08544, USA*

[‡]*Applied Thermodynamics, Department of Mechanical Engineering, Chemnitz University
of Technology, 09126 Chemnitz, Germany*

E-mail: azp@princeton.edu

Supporting Information Available

Model parameters

Interactions consisted of a Lennard-Jones and Coulomb potential, the form of which is given in eq 1.

$$U_{ij} = 4\varepsilon_{ij} \left[\left(\frac{\sigma_{ij}}{r_{ij}} \right)^{12} - \left(\frac{\sigma_{ij}}{r_{ij}} \right)^6 \right] + \frac{q_i q_j}{4\pi\epsilon\epsilon_0 r_{ij}} \quad (1)$$

Cross interactions were obtained from the Lorentz-Berthelot combining rules, given in eqs 2 and 3.

$$\varepsilon_{ij} = \sqrt{\varepsilon_i \varepsilon_j} \quad (2)$$

$$\sigma_{ij} = \frac{1}{2} (\sigma_i + \sigma_j) \quad (3)$$

Interaction parameters for the ion models are listed in Table S1, while interactions for the SPC/E water model are listed in Table S2. The water model was constrained with the SETTLE algorithm with an oxygen-hydrogen distance of 0.1 nm and a hydrogen-hydrogen distance of 0.1633 nm.

Table S1: Ion force field parameters

Force field	$\varepsilon_{\text{Ca}}/\text{kJ}\cdot\text{mol}^{-1}$	$\sigma_{\text{Ca}}/\text{nm}$	q_{Ca}/e	$\varepsilon_{\text{Cl}}/\text{kJ}\cdot\text{mol}^{-1}$	$\sigma_{\text{Cl}}/\text{nm}$	q_{Cl}/e
DRVH	1.662853	0.258	2	1.662853	0.441	-1
Mamatkulov <i>et al.</i>	0.940	0.241	2	0.410	0.440	-1
ECCR2	0.5072	0.26656	1.5	0.4928	0.410	-0.75

Table S2: Water force field parameters

Atom	$\varepsilon/\text{kJ}\cdot\text{mol}^{-1}$	σ/nm	q/e
O	0.6502	0.31655	-0.8476
H	0	0	0.4238

Ideal-gas standard chemical potentials

Table S3: Ideal-gas standard chemical potentials for calcium ($\mu_{\text{Ca}^{2+}}^0$) and chloride ($\mu_{\text{Cl}^-}^0$) ions at different temperatures (T). Values are interpolated from NIST-JANAF thermochemical tables with corrections for ionization of Ca^+ to Ca^{2+} .

T/K	$\mu_{\text{Ca}^{2+}}^0/\text{kJ}\cdot\text{mol}^{-1}$	$\mu_{\text{Cl}^-}^0/\text{kJ}\cdot\text{mol}^{-1}$
298.15	1879.19	-240.167
373.15	1868.99	-241.580
473.15	1855.03	-243.059

Implicit-solvent simulations: extrapolation to infinite system size

For the implicit-solvent simulations, the chemical potential was calculated from eq 4.

$$\mu_{\text{CaCl}_2} = RT \ln \left(\frac{N_{\text{CaCl}_2} \Lambda_{\text{Ca}^{2+}}^3}{V} \right) + 2RT \ln \left(\frac{2N_{\text{CaCl}_2} \Lambda_{\text{Cl}^-}^3}{V} \right) + \mu_{\text{vdw}}^{\text{R}} + \mu_{\text{coul}}^{\text{R}} \quad (4)$$

Λ is the thermal de Broglie wavelength defined as

$$\Lambda = \sqrt{\frac{h^2}{2\pi m k T}} \quad (5)$$

where h is Plank's constant and m is the mass of the atom.

Table S4: Extrapolation to infinite system size for implicit-solvent simulations of DRVH model at 298.15 K and a concentration of 0.0066 mol·L⁻¹.

L^a/nm	$N_{\text{CaCl}_2}^b$	$\mu_{\text{CaCl}_2}^c/\text{kJ}\cdot\text{mol}^{-1}$	$u(\mu_{\text{CaCl}_2})/\text{kJ}\cdot\text{mol}^{-1}$
5	0.5	-132.81	0.06
7.21125	1.5	-132.25	0.06
9.56466	3.5	-131.99	0.06
12.33106	7.5	-131.87	0.02
∞		-131.18	0.07

^a Side length of simulation box

^b Number of CaCl₂ molecules at midpoint of ion insertion

^c Chemical potential of CaCl₂

Table S5: Extrapolation to infinite system size for implicit-solvent simulations of DRVH model at 298.15 K and a concentration of 0.020 mol·L⁻¹.

L^a/nm	$N_{\text{CaCl}_2}^b$	$\mu_{\text{CaCl}_2}^c/\text{kJ}\cdot\text{mol}^{-1}$	$u(\mu_{\text{CaCl}_2})/\text{kJ}\cdot\text{mol}^{-1}$
5	1.5	-125.71	0.05
7.71011	5.5	-125.35	0.03
10.13700	12.5	-125.22	0.05
12.5111	23.5	-125.23	0.04
∞		-124.84	0.07

^a Side length of simulation box

^b Number of CaCl₂ molecules at midpoint of ion insertion

^c Chemical potential of CaCl₂

Table S6: Extrapolation to infinite system size for implicit-solvent simulations of DRVH model at 298.15 K and a concentration of 0.033 mol·L⁻¹.

L^a/nm	$N_{\text{CaCl}_2}^b$	$\mu_{\text{CaCl}_2}^c/\text{kJ}\cdot\text{mol}^{-1}$	$u(\mu_{\text{CaCl}_2})/\text{kJ}\cdot\text{mol}^{-1}$
5	2.5	-122.66	0.05
7.51847	8.5	-122.48	0.03
10.08265	20.5	-122.36	0.04
12.54649	39.5	-122.30	0.04
∞		-122.06	0.06

^a Side length of simulation box

^b Number of CaCl₂ molecules at midpoint of ion insertion

^c Chemical potential of CaCl₂

Table S7: Extrapolation to infinite system size for implicit-solvent simulations of DRVH model at 298.15 K and a concentration of 0.073 mol·L⁻¹.

L^a/nm	$N_{\text{CaCl}_2}^b$	$\mu_{\text{CaCl}_2}^c/\text{kJ}\cdot\text{mol}^{-1}$	$u(\mu_{\text{CaCl}_2})/\text{kJ}\cdot\text{mol}^{-1}$
5	5.5	-118.44	0.06
7.49157	18.5	-118.26	0.07
10.03774	44.5	-118.29	0.02
12.47875	85.5	-118.28	0.03
∞		-118.15	0.06

^a Side length of simulation box

^b Number of CaCl₂ molecules at midpoint of ion insertion

^c Chemical potential of CaCl₂

Table S8: Extrapolation to infinite system size for implicit-solvent simulations of DRVH model at 298.15 K and a concentration of 0.139 mol·L⁻¹.

L^a/nm	$N_{\text{CaCl}_2}^b$	$\mu_{\text{CaCl}_2}^c/\text{kJ}\cdot\text{mol}^{-1}$	$u(\mu_{\text{CaCl}_2})/\text{kJ}\cdot\text{mol}^{-1}$
5	10.5	-115.32	0.04
7.50441	35.5	-115.25	0.05
10.0198	84.5	-115.25	0.05
12.5111	164.5	-115.27	0.05
∞		-115.21	0.08

^a Side length of simulation box

^b Number of CaCl₂ molecules at midpoint of ion insertion

^c Chemical potential of CaCl₂

Table S9: Slope of extrapolation to infinite system size at different concentrations (m) for DRVH CaCl₂ model in implicit solvent. Standard uncertainty is $u(\text{slope}) = 0.5 \text{ kJ}\cdot\text{nm}\cdot\text{mol}^{-1}$.

$m/\text{mol}\cdot\text{L}^{-1}$	slope/ $\text{kJ}\cdot\text{nm}\cdot\text{mol}^{-1}$
0.0066	-8.0
0.020	-4.2
0.033	-3.1
0.073	-1.3
0.139	-0.5

Explicit-solvent simulations: extrapolation to infinite system size and infinite dilution

Table S10: Extrapolation to infinite system size for the DRVH model at 298.15 K, 1 bar, and a concentration of 0.056 mol·kg⁻¹.

N_{CaCl_2} ^a	$N_{\text{H}_2\text{O}}$ ^b	L^c/nm	$u(L)/\text{nm}$	$\mu_{\text{CaCl}_2}^d/\text{kJ}\cdot\text{mol}^{-1}$	$u(\mu_{\text{CaCl}_2})/\text{kJ}\cdot\text{mol}^{-1}$
0.5	500	2.4665	0.0001	-709.2	0.2
1.5	1500	3.5573	0.0001	-707.9	0.1
2.5	2500	4.21767	0.00008	-708.2	0.3
5.5	5500	5.48557	0.00002	-707.9	0.3
		∞		-706.8	0.4

^a Number of CaCl₂ molecules at midpoint of ion insertion

^b Number of water molecules ^c Side length of simulation box

^d Chemical potential of CaCl₂

Table S11: Extrapolation to infinite system size for the Mamatkulov *et al.* model at 298.15 K, 1 bar, and a concentration of 0.056 mol·kg⁻¹.

N_{CaCl_2} ^a	$N_{\text{H}_2\text{O}}$ ^b	L^c/nm	$u(L)/\text{nm}$	$\mu_{\text{CaCl}_2}^d/\text{kJ}\cdot\text{mol}^{-1}$	$u(\mu_{\text{CaCl}_2})/\text{kJ}\cdot\text{mol}^{-1}$
0.5	500	2.46585	0.00008	-836.4	0.2
1.5	1500	3.55629	0.00006	-835.3	0.1
2.5	2500	4.21633	0.00005	-834.6	0.1
5.5	5500	5.48372	0.00004	-835.1	0.4
		∞		-833.5	0.6

^a Number of CaCl₂ molecules at midpoint of ion insertion

^b Number of water molecules ^c Side length of simulation box

^d Chemical potential of CaCl₂

Table S12: Extrapolation to infinite system size for the ECCR2 model at 298.15 K, 1 bar, and a concentration of 0.056 mol·kg⁻¹.

N_{CaCl_2} ^a	$N_{\text{H}_2\text{O}}$ ^b	L^c/nm	$u(L)/\text{nm}$	$\mu_{\text{CaCl}_2}^d/\text{kJ}\cdot\text{mol}^{-1}$	$u(\mu_{\text{CaCl}_2})/\text{kJ}\cdot\text{mol}^{-1}$
0.5	500	2.46755	0.00005	171.5	0.2
1.5	1500	3.55866	0.00004	172.0	0.1
2.5	2500	4.21915	0.00003	172.3	0.1
5.5	5500	5.48738	0.00003	172.6	0.2
		∞		173.6	0.3

^a Number of CaCl₂ molecules at midpoint of ion insertion

^b Number of water molecules ^c Side length of simulation box

^d Chemical potential of CaCl₂

Table S13: Extrapolation to infinite system size for the DRVH model at 373.15 K, 1 bar, and a concentration of 0.056 mol·kg⁻¹.

N_{CaCl_2} ^a	$N_{\text{H}_2\text{O}}$ ^b	L^c/nm	$u(L)/\text{nm}$	$\mu_{\text{CaCl}_2}^d/\text{kJ}\cdot\text{mol}^{-1}$	$u(\mu_{\text{CaCl}_2})/\text{kJ}\cdot\text{mol}^{-1}$
0.5	500	2.51155	0.00008	-688.6	0.1
1.5	1500	3.62201	0.00003	-687.5	0.1
2.5	2500	4.29438	0.00002	-686.9	0.2
5.5	5500	5.58516	0.00005	-686.5	0.5
		∞		-684.8	0.6

^a Number of CaCl₂ molecules at midpoint of ion insertion

^b Number of water molecules ^c Side length of simulation box

^d Chemical potential of CaCl₂

Table S14: Extrapolation to infinite system size for the Mamatkulov *et al.* model at 373.15 K, 1 bar, and a concentration of 0.056 mol·kg⁻¹.

N_{CaCl_2} ^a	$N_{\text{H}_2\text{O}}$ ^b	L^c/nm	$u(L)/\text{nm}$	$\mu_{\text{CaCl}_2}^d/\text{kJ}\cdot\text{mol}^{-1}$	$u(\mu_{\text{CaCl}_2})/\text{kJ}\cdot\text{mol}^{-1}$
0.5	500	2.51076	0.00004	-812.4	0.2
1.5	1500	3.62084	0.00005	-810.8	0.2
2.5	2500	4.29301	0.00004	-810.7	0.3
5.5	5500	5.58336	0.00003	-810.3	0.2
		∞		-808.4	0.3

^a Number of CaCl₂ molecules at midpoint of ion insertion

^b Number of water molecules ^c Side length of simulation box

^d Chemical potential of CaCl₂

Table S15: Extrapolation to infinite system size for the ECCR2 model at 373.15 K, 1 bar, and a concentration of 0.056 mol·kg⁻¹.

N_{CaCl_2} ^a	$N_{\text{H}_2\text{O}}$ ^b	L^c/nm	$u(L)/\text{nm}$	$\mu_{\text{CaCl}_2}^d/\text{kJ}\cdot\text{mol}^{-1}$	$u(\mu_{\text{CaCl}_2})/\text{kJ}\cdot\text{mol}^{-1}$
0.5	500	2.51262	0.00005	178.5	0.1
1.5	1500	3.62358	0.00005	179.7	0.2
2.5	2500	4.29616	0.00004	180.1	0.3
5.5	5500	5.58753	0.00002	180.0	0.4
		∞		181.6	0.5

^a Number of CaCl₂ molecules at midpoint of ion insertion

^b Number of water molecules ^c Side length of simulation box

^d Chemical potential of CaCl₂

Table S16: Extrapolation to infinite system size for the DRVH model at 473.15 K, 15.5 bar, and a concentration of 0.056 mol·kg⁻¹.

N_{CaCl_2} ^a	$N_{\text{H}_2\text{O}}$ ^b	L^c/nm	$u(L)/\text{nm}$	$\mu_{\text{CaCl}_2}^d/\text{kJ}\cdot\text{mol}^{-1}$	$u(\mu_{\text{CaCl}_2})/\text{kJ}\cdot\text{mol}^{-1}$
0.5	500	2.61645	0.00007	-654.8	0.1
1.5	1500	3.77283	0.00006	-653.3	0.2
2.5	2500	4.4730	0.0001	-652.9	0.2
5.5	5500	5.81748	0.00007	-652.1	0.4
		∞		-650.0	0.5

^a Number of CaCl₂ molecules at midpoint of ion insertion

^b Number of water molecules ^c Side length of simulation box

^d Chemical potential of CaCl₂

Table S17: Extrapolation to infinite system size for the Mamatkulov *et al.* model at 473.15 K, 15.5 bar, and a concentration of 0.056 mol·kg⁻¹.

N_{CaCl_2} ^a	$N_{\text{H}_2\text{O}}$ ^b	L^c/nm	$u(L)/\text{nm}$	$\mu_{\text{CaCl}_2}^d/\text{kJ}\cdot\text{mol}^{-1}$	$u(\mu_{\text{CaCl}_2})/\text{kJ}\cdot\text{mol}^{-1}$
0.5	500	2.61572	0.00009	-775.5	0.2
1.5	1500	3.77193	0.00006	-774.0	0.2
2.5	2500	4.4719	0.0001	-773.1	0.1
5.5	5500	5.81618	0.00005	-772.8	0.2
		∞		-770.3	0.3

^a Number of CaCl₂ molecules at midpoint of ion insertion

^b Number of water molecules ^c Side length of simulation box

^d Chemical potential of CaCl₂

Table S18: Extrapolation to infinite system size for the ECCR2 model at 473.15 K, 15.5 bar, and a concentration of 0.056 mol·kg⁻¹.

N_{CaCl_2} ^a	$N_{\text{H}_2\text{O}}$ ^b	L^c/nm	$u(L)/\text{nm}$	$\mu_{\text{CaCl}_2}^d/\text{kJ}\cdot\text{mol}^{-1}$	$u(\mu_{\text{CaCl}_2})/\text{kJ}\cdot\text{mol}^{-1}$
0.5	500	2.6185	0.0001	192.1	0.1
1.5	1500	3.77595	0.00007	193.3	0.1
2.5	2500	4.47670	0.00007	193.8	0.1
5.5	5500	5.82218	0.00008	193.9	0.3
		∞		195.7	0.3

^a Number of CaCl₂ molecules at midpoint of ion insertion

^b Number of water molecules ^c Side length of simulation box

^d Chemical potential of CaCl₂

Table S19: Extrapolation to infinite dilution and infinite system size for the DRVH model at 298.15 K and 1 bar.

N_{CaCl_2} ^a	$N_{\text{H}_2\text{O}}$ ^b	L^c/nm	$u(L)/\text{nm}$	$\mu_{\text{CaCl}_2}^{\text{R}d}/\text{kJ}\cdot\text{mol}^{-1}$	$u(\mu_{\text{CaCl}_2}^{\text{R}})/\text{kJ}\cdot\text{mol}^{-1}$
0.5	500	2.4665	0.0001	-2113.8	0.2
0.5	1500	3.55560	0.00004	-2112.3	0.1
0.5	2500	4.21529	0.00005	-2111.7	0.3
0.5	5500	5.48184	0.00004	-2110.9	0.2
		∞		-2108.5	0.3

^a Number of CaCl_2 molecules at midpoint of ion insertion

^b Number of water molecules ^c Side length of simulation box

^d Residual chemical potential of CaCl_2

Table S20: Extrapolation to infinite dilution and infinite system size for the Mamatkulov *et al.* model at 298.15 K and 1 bar.

N_{CaCl_2} ^a	$N_{\text{H}_2\text{O}}$ ^b	L^c/nm	$u(L)/\text{nm}$	$\mu_{\text{CaCl}_2}^{\text{R}d}/\text{kJ}\cdot\text{mol}^{-1}$	$u(\mu_{\text{CaCl}_2}^{\text{R}})/\text{kJ}\cdot\text{mol}^{-1}$
0.5	500	2.46585	0.00008	-2241.0	0.2
0.5	1500	3.55450	0.00005	-2239.2	0.1
0.5	2500	4.21403	0.00004	-2238.5	0.1
0.5	5500	5.48049	0.00003	-2238.0	0.5
		∞		-2235.3	0.6

^a Number of CaCl_2 molecules at midpoint of ion insertion

^b Number of water molecules ^c Side length of simulation box

^d Residual chemical potential of CaCl_2

Table S21: Extrapolation to infinite dilution and infinite system size for the ECCR2 model at 298.15 K and 1 bar.

N_{CaCl_2} ^a	$N_{\text{H}_2\text{O}}$ ^b	L^c/nm	$u(L)/\text{nm}$	$\mu_{\text{CaCl}_2}^{\text{R}d}/\text{kJ}\cdot\text{mol}^{-1}$	$u(\mu_{\text{CaCl}_2}^{\text{R}})/\text{kJ}\cdot\text{mol}^{-1}$
0.5	500	2.46755	0.00005	-1233.1	0.2
0.5	1500	3.55610	0.00006	-1232.1	0.1
0.5	2500	4.21554	0.00005	-1232.1	0.3
0.5	5500	5.48201	0.00002	-1231.6	0.3
		∞		-1230.4	0.5

^a Number of CaCl_2 molecules at midpoint of ion insertion

^b Number of water molecules ^c Side length of simulation box

^d Residual chemical potential of CaCl_2

Table S22: Extrapolation to infinite dilution and infinite system size for the DRVH model at 373.15 K and 1 bar.

N_{CaCl_2} ^a	$N_{\text{H}_2\text{O}}$ ^b	L^c/nm	$u(L)/\text{nm}$	$\mu_{\text{CaCl}_2}^{\text{R}d}/\text{kJ}\cdot\text{mol}^{-1}$	$u(\mu_{\text{CaCl}_2}^{\text{R}})/\text{kJ}\cdot\text{mol}^{-1}$
0.5	500	2.51155	0.00008	-2083.2	0.1
0.5	1500	3.62074	0.00004	-2081.0	0.1
0.5	2500	4.29253	0.00004	-2080.2	0.2
0.5	5500	5.58251	0.00004	-2079.2	0.1
		∞		-2075.9	0.2

^a Number of CaCl_2 molecules at midpoint of ion insertion

^b Number of water molecules ^c Side length of simulation box

^d Residual chemical potential of CaCl_2

Table S23: Extrapolation to infinite dilution and infinite system size for the Mamatkulov *et al.* model at 373.15 K and 1 bar.

N_{CaCl_2} ^a	$N_{\text{H}_2\text{O}}$ ^b	L^c/nm	$u(L)/\text{nm}$	$\mu_{\text{CaCl}_2}^{\text{R}d}/\text{kJ}\cdot\text{mol}^{-1}$	$u(\mu_{\text{CaCl}_2}^{\text{R}})/\text{kJ}\cdot\text{mol}^{-1}$
0.5	500	2.51076	0.00004	-2207.0	0.2
0.5	1500	3.61933	0.00006	-2204.7	0.1
0.5	2500	4.29106	0.00004	-2203.6	0.3
0.5	5500	5.58076	0.00003	-2202.3	0.4
		∞		-2198.5	0.6

^a Number of CaCl_2 molecules at midpoint of ion insertion

^b Number of water molecules ^c Side length of simulation box

^d Residual chemical potential of CaCl_2

Table S24: Extrapolation to infinite dilution and infinite system size for the ECCR2 model at 373.15 K and 1 bar.

N_{CaCl_2} ^a	$N_{\text{H}_2\text{O}}$ ^b	L^c/nm	$u(L)/\text{nm}$	$\mu_{\text{CaCl}_2}^{\text{R}d}/\text{kJ}\cdot\text{mol}^{-1}$	$u(\mu_{\text{CaCl}_2}^{\text{R}})/\text{kJ}\cdot\text{mol}^{-1}$
0.5	500	2.51262	0.00005	-1216.2	0.1
0.5	1500	3.62121	0.00006	-1214.7	0.1
0.5	2500	4.29293	0.00006	-1214.1	0.2
0.5	5500	5.58281	0.00003	-1213.5	0.2
		∞		-1211.3	0.3

^a Number of CaCl_2 molecules at midpoint of ion insertion

^b Number of water molecules ^c Side length of simulation box

^d Residual chemical potential of CaCl_2

Table S25: Extrapolation to infinite dilution and infinite system size for the DRVH model at 473.15 K and 15.5 bar.

N_{CaCl_2} ^a	$N_{\text{H}_2\text{O}}$ ^b	L^c/nm	$u(L)/\text{nm}$	$\mu_{\text{CaCl}_2}^{\text{R}d}/\text{kJ}\cdot\text{mol}^{-1}$	$u(\mu_{\text{CaCl}_2}^{\text{R}})/\text{kJ}\cdot\text{mol}^{-1}$
0.5	500	2.61645	0.00007	-2036.3	0.1
0.5	1500	3.77372	0.00008	-2032.6	0.2
0.5	2500	4.47434	0.00008	-2031.4	0.2
0.5	5500	5.81947	0.00003	-2029.2	0.2
		∞		-2023.8	0.3

^a Number of CaCl_2 molecules at midpoint of ion insertion

^b Number of water molecules ^c Side length of simulation box

^d Residual chemical potential of CaCl_2

Table S26: Extrapolation to infinite dilution and infinite system size for the Mamatkulov *et al.* model at 473.15 K and 15.5 bar.

N_{CaCl_2} ^a	$N_{\text{H}_2\text{O}}$ ^b	L^c/nm	$u(L)/\text{nm}$	$\mu_{\text{CaCl}_2}^{\text{R}d}/\text{kJ}\cdot\text{mol}^{-1}$	$u(\mu_{\text{CaCl}_2}^{\text{R}})/\text{kJ}\cdot\text{mol}^{-1}$
0.5	500	2.61572	0.00009	-2157.0	0.2
0.5	1500	3.7735	0.0001	-2152.8	0.1
0.5	2500	4.47411	0.00006	-2150.9	0.3
0.5	5500	5.81939	0.00008	-2149.6	0.3
		∞		-2143.2	0.4

^a Number of CaCl_2 molecules at midpoint of ion insertion

^b Number of water molecules ^c Side length of simulation box

^d Residual chemical potential of CaCl_2

Table S27: Extrapolation to infinite dilution and infinite system size for the ECCR2 model at 473.15 K and 15.5 bar.

N_{CaCl_2} ^a	$N_{\text{H}_2\text{O}}$ ^b	L^c/nm	$u(L)/\text{nm}$	$\mu_{\text{CaCl}_2}^{\text{R}d}/\text{kJ}\cdot\text{mol}^{-1}$	$u(\mu_{\text{CaCl}_2}^{\text{R}})/\text{kJ}\cdot\text{mol}^{-1}$
0.5	500	2.6185	0.0001	-1189.3	0.1
0.5	1500	3.7748	0.0001	-1187.7	0.2
0.5	2500	4.4751	0.0001	-1186.5	0.3
0.5	5500	5.8199	0.0001	-1185.7	0.1
		∞		-1182.7	0.3

^a Number of CaCl_2 molecules at midpoint of ion insertion

^b Number of water molecules ^c Side length of simulation box

^d Residual chemical potential of CaCl_2

Explicit-solvent simulations: chemical potential

Table S28: Chemical potential for CaCl₂ force fields at 298.15 K and 1 bar in SPC/E water.

N_{CaCl_2} ^a per 500 H ₂ O		DRVH		Mamatkulov <i>et al.</i>		ECCR2	
	$m^b/\text{mol}\cdot\text{kg}^{-1}$	$\mu_{\text{CaCl}_2}^c$	$u(\mu_{\text{CaCl}_2})$	μ_{CaCl_2}	$u(\mu_{\text{CaCl}_2})$	μ_{CaCl_2}	$u(\mu_{\text{CaCl}_2})$
0.5	0.056	-706.8	0.4	-833.5	0.6	173.6	0.3
4.5	0.50	-693.6	0.2	-820.8	0.1	188.5	0.1
8.5	0.94	-688.0	0.2	-815.3	0.2	194.6	0.2
17.5	1.94	-678.7	0.1	-807.0	0.1	202.3	0.2
26.5	2.94	-670.0	0.2	-799.7	0.2	208.6	0.1
35.5	3.94	-660.9	0.3			213.2	0.1
44.5	4.94	-654.6	0.3			217.3	0.2
53.5	5.94	-651.3	0.3			221.6	0.2
62.5	6.94	-651.9	0.4			225.0	0.1

^a Number of calcium chloride molecules at midpoint of ion insertion

^b Concentration of CaCl₂ in water ^c Chemical potential of CaCl₂

Table S29: Chemical potential for CaCl₂ force fields at 373.15 K and 1 bar in SPC/E water.

N_{CaCl_2} ^a per 500 H ₂ O		DRVH		Mamatkulov <i>et al.</i>		ECCR2	
	$m^b/\text{mol}\cdot\text{kg}^{-1}$	$\mu_{\text{CaCl}_2}^c$	$u(\mu_{\text{CaCl}_2})$	μ_{CaCl_2}	$u(\mu_{\text{CaCl}_2})$	μ_{CaCl_2}	$u(\mu_{\text{CaCl}_2})$
0.5	0.056	-684.8	0.6	-808.4	0.3	181.6	0.5
4.5	0.50	-669.6	0.1	-793.9	0.2	199.5	0.1
8.5	0.94	-663.2	0.1	-788.1	0.1	206.4	0.1
17.5	1.94	-652.8	0.1	-779.8	0.3	216.0	0.2
26.5	2.94	-643.3	0.1	-772.8	0.2	222.5	0.1
35.5	3.94	-636.2	0.5	-772.5	0.7	227.9	0.1
44.5	4.94	-623.8	0.4	-762.7	0.3	231.8	0.1
53.5	5.94	-614.1	0.4			236.7	0.1
62.5	6.94	-611.8	0.4			240.4	0.3

^a Number of calcium chloride molecules at midpoint of ion insertion

^b Concentration of CaCl₂ in water ^c Chemical potential of CaCl₂

Table S30: Chemical potential for CaCl₂ force fields at 473.15 K and 15.5 bar in SPC/E water.

N_{CaCl_2} ^a per 500 H ₂ O	m^b /mol·kg ⁻¹	DRVH		Mamatkulov <i>et al.</i>		ECCR2	
		μ_{CaCl_2} ^c	$u(\mu_{\text{CaCl}_2})$	μ_{CaCl_2}	$u(\mu_{\text{CaCl}_2})$	μ_{CaCl_2}	$u(\mu_{\text{CaCl}_2})$
0.5	0.056	-650.0	0.5	-770.3	0.3	195.7	0.3
4.5	0.50	-633.8	0.3	-756.3	0.1	216.8	0.1
8.5	0.94	-627.0	0.1	-751.3	0.2	224.8	0.2
17.5	1.94	-616.8	0.2	-744.8	0.2	235.2	0.2
26.5	2.94	-607.5	0.2	-740.9	0.3	242.0	0.1
35.5	3.94	-598.1	0.1	-737.6	0.2	247.1	0.1
44.5	4.94	-588.8	0.2	-734.6	0.2	251.7	0.2
53.5	5.94	-579.1	0.3	-730.7	0.4	257.0	0.2
62.5	6.94	-570.1	0.4	-727.5	0.3	260.8	0.1

^a Number of calcium chloride molecules at midpoint of ion insertion

^b Concentration of CaCl₂ in water ^c Chemical potential of CaCl₂

Fit parameters for activity coefficients

Table S31: The parameters used to fit the activity coefficients at 298.15 K and 1 bar.

Force field	B	C	D	E
DRVH	4.932	-0.2197	0.3476	-0.03658
Mamatkulov <i>et al.</i>	8.476	-1.053	0.8583	-0.1431
ECCR2	6.977	0.2106	0.04770	0.004258
Mamatkulov <i>et al.</i> from Ref. S1	3.00085	0.41228	0	0

Table S32: The parameters used to fit the activity coefficients at 373.15 K and 1 bar.

Force field	B	C	D	E
DRVH	6.837	-0.5590	0.3571	-0.02963
Mamatkulov <i>et al.</i>	6.447	-1.140	0.7507	-0.1197
ECCR2	4.085	0.2465	0.01563	0.001570
Mamatkulov <i>et al.</i> from Ref. S1 (365 K, 275 bar)	27700.7	0.22039	0	0

Table S33: The parameters used to fit the activity coefficients at 473.15 K and 1 bar.

Force field	B	C	D	E
DRVH	3.943	-0.2909	0.1872	-0.01240
Mamatkulov <i>et al.</i>	3.178	-0.3586	0.08752	-0.005228
ECCR2	4.958	0.02249	0.04054	-0.002886

Comparison of activity coefficients with literature

It is possible to calculate activity coefficients from the values for μ_{CaCl_2} and $\mu_{\text{CaCl}_2}^\dagger$ in Moučka *et al.* for the Mamatkulov *et al.* force field.^{S1} These are compared with our results in Figures S1 and S2. The results from Moučka *et al.* have higher uncertainty and are systematically above the results from this work due to the different values for $\mu_{\text{CaCl}_2}^\dagger$. The fits to the Moučka *et al.* are drawn using the parameters given in ref S1.

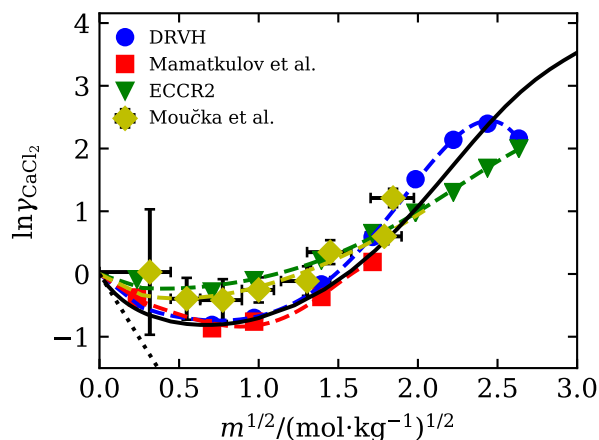


Figure S1: Activity coefficients for the three CaCl_2 force fields at 298.15 K and 1 bar. The solid line represents experimental results, while the dashed line shows the Debye-Hückel limiting slope ($-A$) for the experimental water dielectric constant. Literature values calculated from Moučka *et al.*^{S1} are shown for comparison.

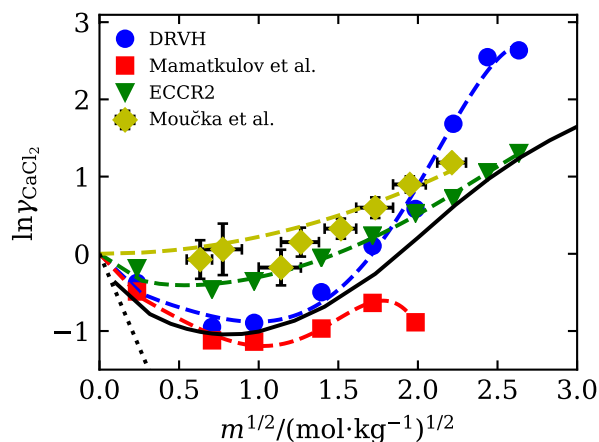


Figure S2: Activity coefficients for the three CaCl_2 force fields at 373.15 K and 1 bar. The solid line represents experimental results, while the dashed line shows the Debye-Hückel limiting slope ($-A$) for the experimental water dielectric constant. Literature values calculated from Moučka *et al.*^{S1} at 365 K and 275 bar are shown for comparison.

Comparison of chemical potential with literature

Despite the difference in state points, the chemical potential for the Mamatkulov *et al.* force field calculated in this work at 373.15 K and 1 bar is similar to that in Moučka *et al.* at 365 K and 275 bar.^{S1} Deviations are only seen in the highest concentration value, at which the chemical potential in this work begins to level out.

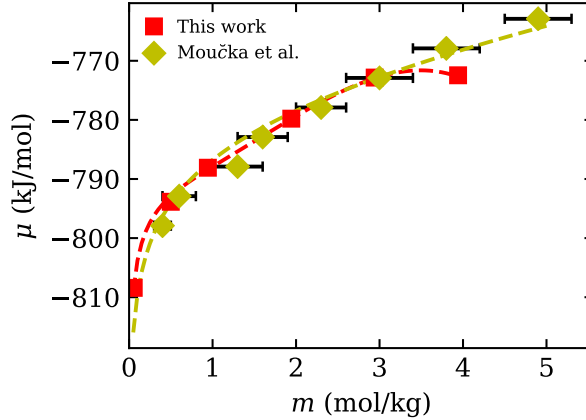


Figure S3: Comparison for the Mamatkulov *et al.* model between chemical potential calculations in this work at 373.15 K and 1 bar and those in Moučka *et al.* at 365 K and 275 bar.^{S1} Error bars indicate one standard error and are not displayed when smaller than points.

Methods to calculate $\mu_{\text{CaCl}_2}^\dagger$

The solution reference chemical potentials ($\mu_{\text{CaCl}_2}^\dagger$) in this work were calculated from eq 6.

$$\mu_{\text{CaCl}_2}^\dagger = \mu_{\text{Ca}^{2+}}^0 + 2\mu_{\text{Cl}^-}^0 + 3RT \ln \left(\frac{kT M_{\text{H}_2\text{O}}}{P^0 v_{\text{H}_2\text{O}}} \right) + \mu_{\text{CaCl}_2}^{\text{R},\infty} \quad (6)$$

Another method for calculating the reference chemical potential is by fitting the activity coefficients to an analytical expression at low concentrations.^{S2-S4} For example, fitting the activity coefficient to the Davies equation^{S5} would give $\mu_{\text{CaCl}_2}^\dagger$ as in eq 7. Since the Davies equation is only valid at low concentrations, the lowest concentration point should be used for the fit.

$$\mu_{\text{CaCl}_2}^\dagger = \mu_{\text{CaCl}_2} - 3RT \ln(\sqrt[3]{4m}) + 3RTA \left(\frac{\sqrt{I}}{1 + \sqrt{I}} - 0.2I \right) \quad (7)$$

A final method that has been used in the past to calculate $\mu_{\text{CaCl}_2}^\dagger$, is by using it as a fitting parameter in eq 8.^{S1,S6}

$$\mu_{\text{CaCl}_2} = \mu_{\text{CaCl}_2}^\dagger + 3RT \ln(\sqrt[3]{4m}) + 3RT \left(-\frac{A\sqrt{I}}{1 + B\sqrt{m}} + Cm + Dm^2 + Em^3 \right) \quad (8)$$

It is also common to leave out the higher order terms in eq 8, giving eq 9 and 10.

$$\mu_{\text{CaCl}_2} = \mu_{\text{CaCl}_2}^\dagger + 3RT \ln(\sqrt[3]{4m}) + 3RT \left(-\frac{A\sqrt{I}}{1 + B\sqrt{m}} + Cm + Dm^2 \right) \quad (9)$$

$$\mu_{\text{CaCl}_2} = \mu_{\text{CaCl}_2}^\dagger + 3RT \ln(\sqrt[3]{4m}) + 3RT \left(-\frac{A\sqrt{I}}{1 + B\sqrt{m}} + Cm \right) \quad (10)$$

A comparison of these methods is given in Table S34 for the DRVH force field at 298.15 K and 1 bar. The result from eq 6 is the one given in this paper. The results for $\mu_{\text{CaCl}_2}^\dagger$ as a fitting parameter depends on the number of parameters used in the fit, but can also be a function of the initial guesses. Two examples are given in Table S34 and Figures S4 and S5 of fits that perform similarly but have different parameter values generated from different initial guesses. Equation 10 is not able to fit the chemical potential well. The fits from eqs 8 and 9 perform similarly to each other, although eq 8 is able to slightly better represent the data. The downside with these equations is that they can also overfit the chemical potential, leading to considerably different values of $\mu_{\text{CaCl}_2}^\dagger$ for the two fits in Table S34. The Davies equation gives a value similar to the other methods. However, one additional downside of both the Davies equation and calculating $\mu_{\text{CaCl}_2}^\dagger$ as a fitting parameter is that the uncertainty in the dielectric constant of the water model will influence the accuracy in $\mu_{\text{CaCl}_2}^\dagger$.

Table S34: Reference chemical potential ($\mu_{\text{CaCl}_2}^\dagger$) for the DRVH CaCl_2 force field at 298.15 K and 1 bar using various calculation methods.

Force field	$\mu_{\text{CaCl}_2}^\dagger/\text{kJ}\cdot\text{mol}^{-1}$
Equation 6	-685.8 ± 0.3
Equation 7	-684.3
Fit A from eq 8	-684.4
Fit B from eq 8	-683.0
Fit A from eq 9	-681.8
Fit B from eq 9	-682.5
Fit A from eq 10	-698.3
Fit B from eq 10	-686.3

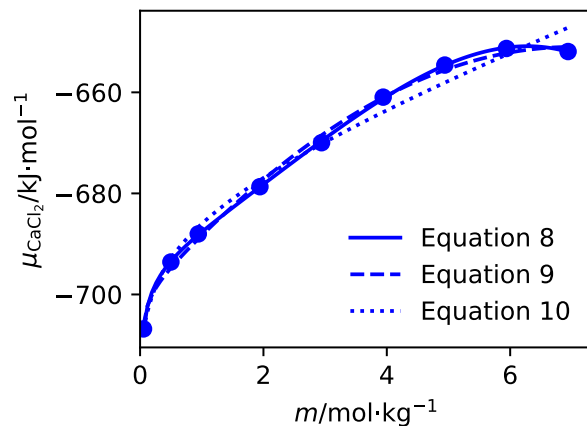


Figure S4: Fit A to the chemical potential for the DRVH model at 298.15 K and 1 bar.

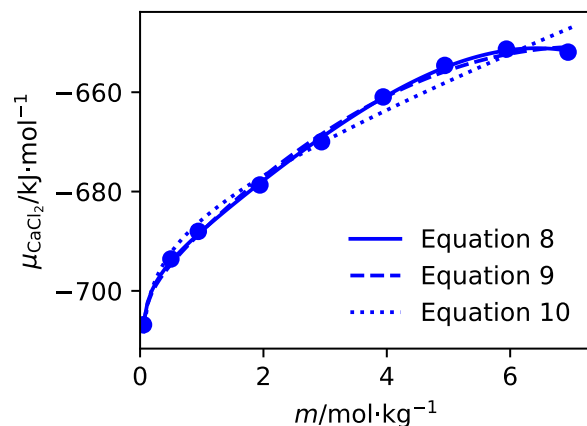


Figure S5: Fit B to the chemical potential for the DRVH model at 298.15 K and 1 bar.

Replica exchange molecular dynamics

Replica exchange molecular dynamics (REMD) simulations were performed to evaluate the accuracy of the quenching method simulations. The replicas were exponentially distributed at 20 temperatures from 298.15 K to 473.15 K. Swaps were attempted every 1 ps. The resulting distribution of the coulomb energy for one ion triplet is compared for the REMD and quenched simulations in Figures S6 and S7 for the DRVH model. At a concentration of 5.00 mol·kg⁻¹, the distributions are identical for both methods. However, at 5.99 mol·kg⁻¹, the distributions begin to differ. The REMD simulations are more expensive than the quenching simulations and require all simulations to run in parallel, so REMD simulations were not used to calculate the chemical potential.

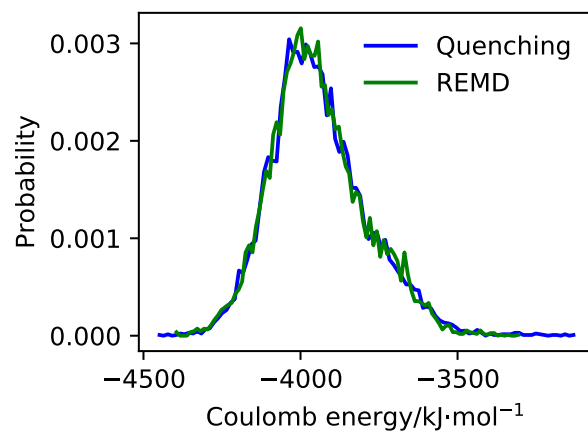


Figure S6: Distribution of the coulomb energy for one CaCl_2 molecule in a $5.00 \text{ mol}\cdot\text{kg}^{-1}$ solution at 298.15 K . Results are for the DRVH force field in SPC/E water.

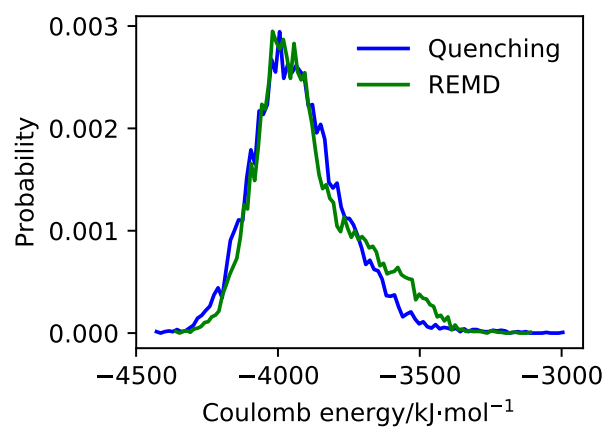


Figure S7: Distribution of the coulomb energy for one CaCl_2 molecule in a $5.99 \text{ mol}\cdot\text{kg}^{-1}$ solution at 298.15 K . Results are for the DRVH force field in SPC/E water.

Hydrate crystal lattice constants and angles

Table S35: Lattice constants (a , b , and c) for three models of CaCl_2 dihydrate with SPC/E water. Experimental values are $a = .5893$ nm, $b = .7469$ nm, and $c = 1.2070$ nm.^{S7}

T/K	DRVH			Mamatkulov <i>et al.</i>			ECCR2		
	a^{a}/nm	b^{a}/nm	c^{a}/nm	a/nm	b/nm	c/nm	a/nm	b/nm	c/nm
298.15	0.651	0.865	1.297	0.610	0.782	1.236	0.618	0.792	1.250
333.15	0.653	0.864	1.300	0.610	0.784	1.237	0.614	0.792	1.247
373.15	0.653	0.866	1.308	0.610	0.784	1.237	0.616	0.795	1.258
413.15	0.652	0.867	1.304	0.610	0.786	1.243	0.615	0.800	1.262
453.15	0.654	0.866	1.280	0.611	0.788	1.247			

^a Standard uncertainty $u(a, b, c) = 0.001$ nm

Table S36: Lattice constants (a , b , and c) and angles (α , β , and γ) for DRVH model of CaCl_2 tetrahydrate with SPC/E water. Experimental values are $a = .65932$ nm, $b = .63673$ nm, $c = .85606$ nm, $\alpha = 97.83^\circ$, $\beta = 93.50^\circ$, and $\gamma = 110.58^\circ$.^{S8}

T/K	a^{a}/nm	b^{a}/nm	c^{a}/nm	$\alpha^{\text{b}/\circ}$	$\beta^{\text{b}/\circ}$	$\gamma^{\text{b}/\circ}$
273.15	0.6917	0.6390	1.0152	96.52	94.97	104.12
298.15	0.6928	0.6407	1.0154	96.55	94.84	104.28
313.15	0.6934	0.6417	1.0157	96.56	94.77	104.37

^a Standard uncertainty $u(a, b, c) = 0.0001$ nm

^b Standard uncertainty $u(\alpha, \beta, \gamma) = 0.01^\circ$

Methods for uncertainty calculation

The uncertainty (u) in the chemical potentials and activity coefficients presented in this work is calculated from five independent simulations of the chemical potential. All uncertainties are given as the standard error, calculated as the sample standard deviation divided by the square root of the number of samples. This error is propagated to the infinite system size chemical potential by assuming that the average chemical potential is normally distributed at each point with a standard deviation given by the standard error. 1,000 samples are then drawn from these distributions, and an extrapolation is fit for each sample. The standard deviation of the extrapolations at $1/L = 0$, or $L = \infty$, is taken as the uncertainty in the infinite system size chemical potential. The uncertainty in L which is given in Tables S10-S27 is neglected in the error propagation since it is considerably smaller than other sources of uncertainty. All other uncertainties are propagated using normal error propagation techniques. For example, the uncertainties in $\ln(\gamma)$ are calculated using eq 11.

$$u(\gamma_{\text{CaCl}_2}) = \frac{1}{3RT} \sqrt{u(\mu_{\text{CaCl}_2})^2 + u(\mu_{\text{CaCl}_2}^\dagger)^2} \quad (11)$$

Since the quenching simulations at high concentrations are too expensive to run independent trials, the uncertainty is calculated from bootstrapping. 1,000 different samples of size 10,000 are drawn with replacement from the data set. The chemical potential for each sample is calculated, and the uncertainty in the average chemical potential is taken as the standard deviation of the samples.

This material is available free of charge via the Internet at <http://pubs.acs.org/>.

Literature Cited

- (S1) Moučka, F.; Kolafa, J.; Lísal, M.; Smith, W. R. Chemical potentials of alkaline earth metal halide aqueous electrolytes and solubility of their hydrates by molecular simulation: Application to CaCl₂, antarcticite, and sinjarite. *J. Chem. Phys.* **2018**, *148*, 222832.
- (S2) Mester, Z.; Panagiotopoulos, A. Z. Mean ionic activity coefficients in aqueous NaCl solutions from molecular dynamics simulations. *J. Chem. Phys.* **2015**, *142*, 044507.
- (S3) Mester, Z.; Panagiotopoulos, A. Z. Temperature-dependent solubilities and mean ionic activity coefficients of alkali halides in water from molecular dynamics simulations. *J. Chem. Phys.* **2015**, *143*, 044505.
- (S4) Young, J. M.; Panagiotopoulos, A. Z. System-size dependence of electrolyte activity coefficients in molecular simulations. *J. Phys. Chem. B* **2018**, *122*, 3330–3338.
- (S5) Davies, C. W. The extent of dissociation of salts in water. Part VIII. An equation for the mean ionic activity coefficient of an electrolyte in water, and a revision of the dissociation constants of some sulphates. *J. Chem. Soc.* **1938**, 2093–2098.
- (S6) Moučka, F.; Nezbeda, I.; Smith, W. R. Molecular simulation of aqueous electrolytes: Water chemical potential results and Gibbs-Duhem equation consistency tests. *J. Chem. Phys.* **2013**, *139*, 124505.

- (S7) Leclaire, A.; Borel, M. M. Le dichlorure de calcium dihydraté. *Acta Crystallogr. B* **1977**, *33*, 1608–1610.
- (S8) Leclaire, A.; Borel, M. M. Liaisons hydrogène et coordination du calcium dans les cristaux de $\text{CaCl}_2 \cdot 4\text{H}_2\text{O}$. *Acta Crystallogr. B* **1979**, *35*, 585–588.